Supplementary Information for: Humanity's Future Capacity for Physical Activity Limited by Climate Change and Population Aging

Haley Staudmyer[1*], Jennifer K. Vanos[2], Ollie Jay[3], Gisel Guzman-Echavarria[2], Qinqin Kong[4], Yudam Hwang[1], Sarah E. Perkins-Kirkpatrick[5,6], Catherine H. Gregory[7,8], Jane W. Baldwin[1]

[1*]Department of Earth System Science, University of California, Irvine, Croul Hall, Irvine, 92697-3100, CA, USA.
[2]School of Sustainability,Arizona State University, 777 E University Dr, Tempe, AZ 85281 , Tempe, 85281, Arizona, USA.
[3]Heat and Health Research Centre, University of Sydney, Western Ave, Camperdown, Sydney, 2006, NSW, Australia.
[4]School of Medicine, Stanford University, 450 Jane Stanford Way, Stanford, 94305, California, USA.
[5]Fenner School of Environment and Society, The Australian National University, 141 Linnaeus Way, Acton, Canberra, 2601, Australian Capital Territory, Australia.
[6]ARC Centre of Excellence for the Weather of the 21st Century, The Australian National University, 141 Linnaeus Way, Acton, Canberra, 2601, Australian Capital Territory, Australia.
[7]University of Bern, Hochschulstrasse 6, Bern, 3012, Switzerland.
[8]Oeschger Centre for Climate Change Research, University of Bern, Hochschulstrasse 4, Bern, 3012, Switzerland.

*Corresponding author(s). E-mail(s): hstaudmy@uci.edu;

1 Supplementary Results

1.1 Warm season M_{max} across age groups and emissions scenarios (Figures S1–S2)

Under SSP5-8.5, children maintain notably higher absolute M_{max} than adults in the midlatitudes and high-elevation areas across all warming levels (e.g., 7.2 vs. 6.0 METs at 4°C in the midlatitudes; Figure S1), reflecting children's near-ceiling baseline values (close to the maximum allowed predicted value of 10 METs; see Online Methods 4.1). However, once warming exceeds approximately 1.5°C and children's M_{max} falls away from this ceiling, its rate of decline in the midlatitudes is no longer smaller than that of adults (−0.56 vs. −0.52 METs/°C, respectively). In hot and tropical environments, children experience faster M_{max} decreases than adults (−0.48 METs/°C in the tropics for children, compared to −0.39 METs/°C for adults). The rates of average warm season M_{max} decrease are similar between the adult and elderly age groups, though slightly smaller in magnitude for both elderly age groups (a global average decrease of −0.48 METs/°C for adults, compared to −0.42 METs/°C and −0.40 METs/°C for old and very old adults, respectively; Figure S1); this pattern holds on a global scale as well as for each latitude band considered.

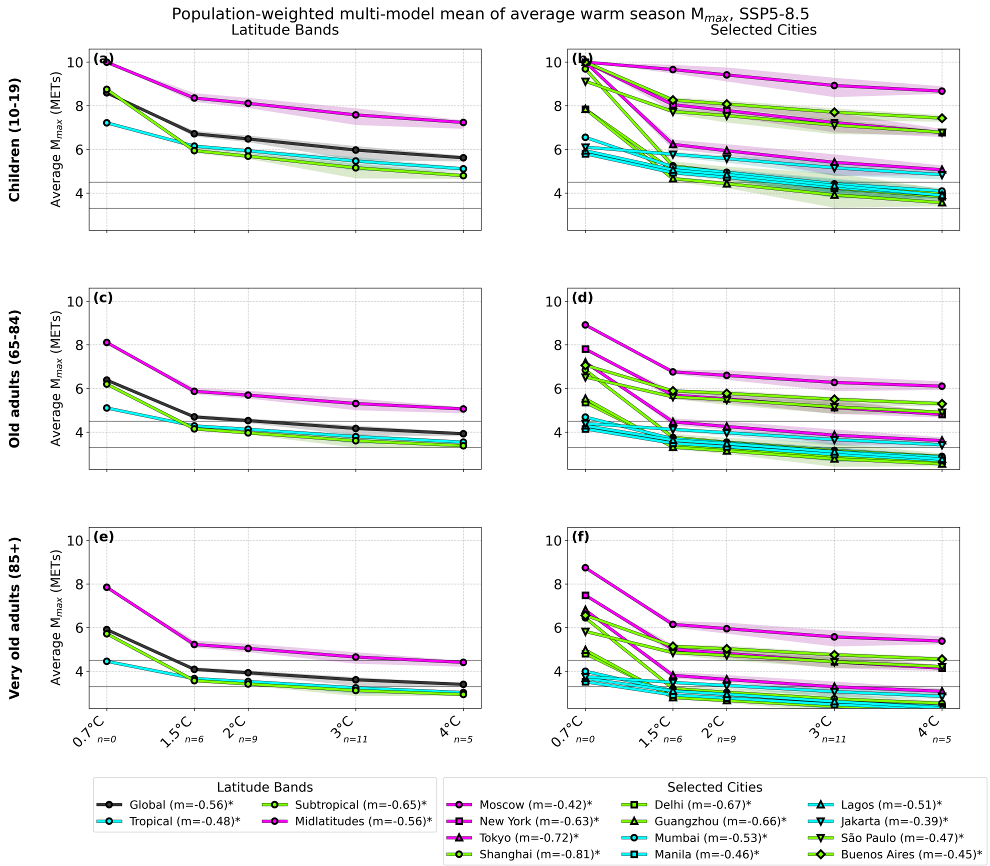

Fig. S1 As in Figure 1, but showing only the latitude-band and city line plots (panels analogous to Figure 1c-d) for three additional age-group profiles – children (10-19; a-b), old adults (65-84; c-d), and very old adults (85+; e-f) – under SSP5-8.5. Adult (20-64) results are featured in Figure 1.

Under the more moderate SSP2-4.5 scenario (Figure S2), the same qualitative age-group ordering holds: children's global average M_{max} declines fastest with warming (-0.64 METs/°C), followed by adults (-0.56 METs/°C), with the two elderly groups declining more slowly and similarly to one another (old adults: -0.51 METs/°C; very old adults: -0.50 METs/°C). Baseline M_{max} values are unchanged from the SSP5-8.5 analysis, since the 1980-2010 ERA5 climatology does not depend on emissions scenario. Because SSP2-4.5 does not reach a 4°C GWL within the models considered in this analysis (Table S2), these slopes are fit over the 0.7–3°C GWL range rather than the full 0.7–4°C range used for SSP5-8.5; direct comparison of slope magnitudes between the two scenarios should therefore be made cautiously.

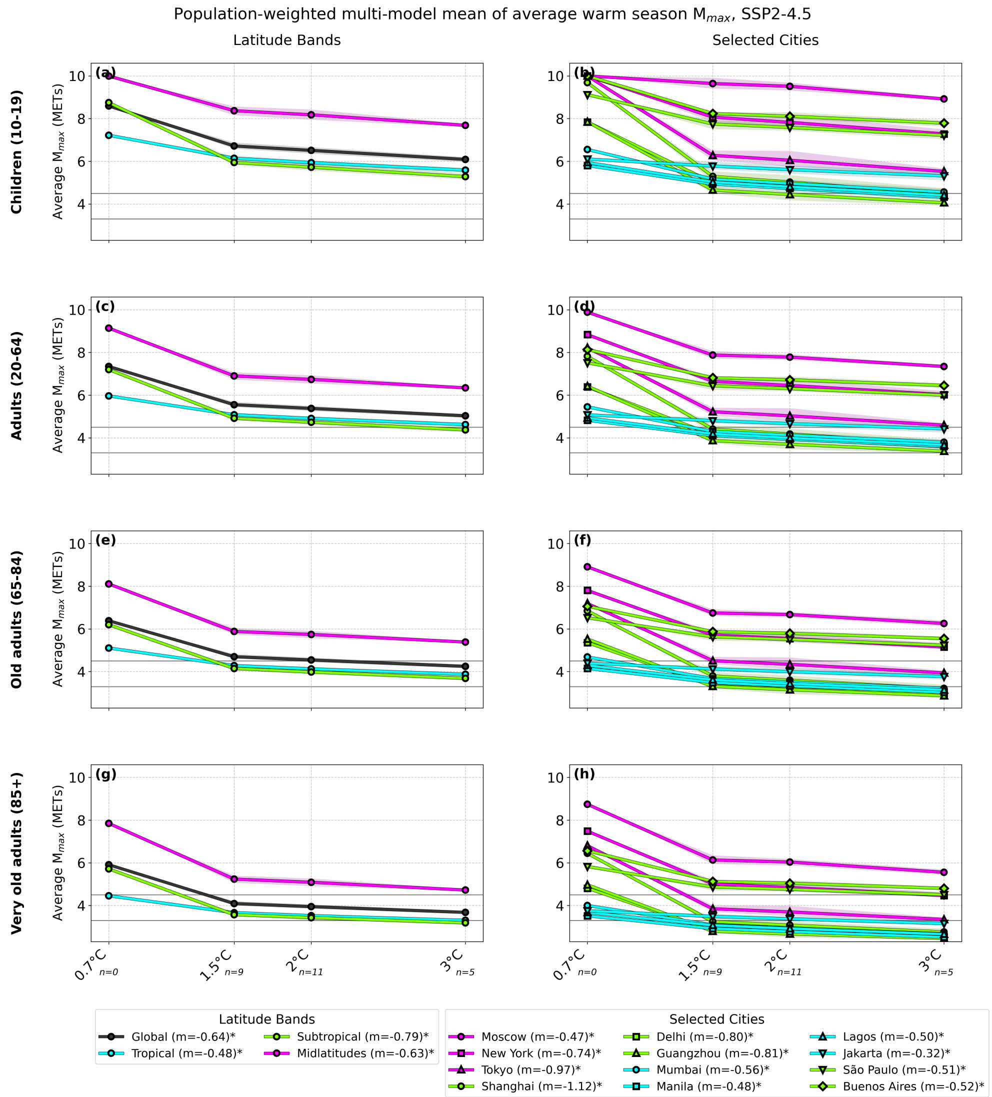

Fig. S2 As in Figure 1, but showing only the latitude-band and city line plots (panels analogous to Figure 1c-d) for all four age-group profiles – children (10-19; a-b), adults (20-64; c-d), old adults (65-84; e-f), and very old adults (85+; g-h) – under SSP2-4.5.

1.2 Time under key M_{max} thresholds across age groups and emissions scenarios (Figures S3–S5)

Under SSP5-8.5, the age-group pattern seen for adults in Figure 2 holds across children, old, and very old adults as well (Figure S3): in the tropics at 2°C GWL, time spent with $M_{max} < 4.8$ METs reaches 13.17% (children), 58.65% (old adults), and 73.20% (very old adults) of the year, compared to 37.69% for adults (Figure 2); for the more stringent $M_{max} < 3.3$ METs threshold, the corresponding tropical values are 0.51%, 12.01%, and 29.72%, compared to 2.87% for adults. This age-group ordering matches Figure 3.

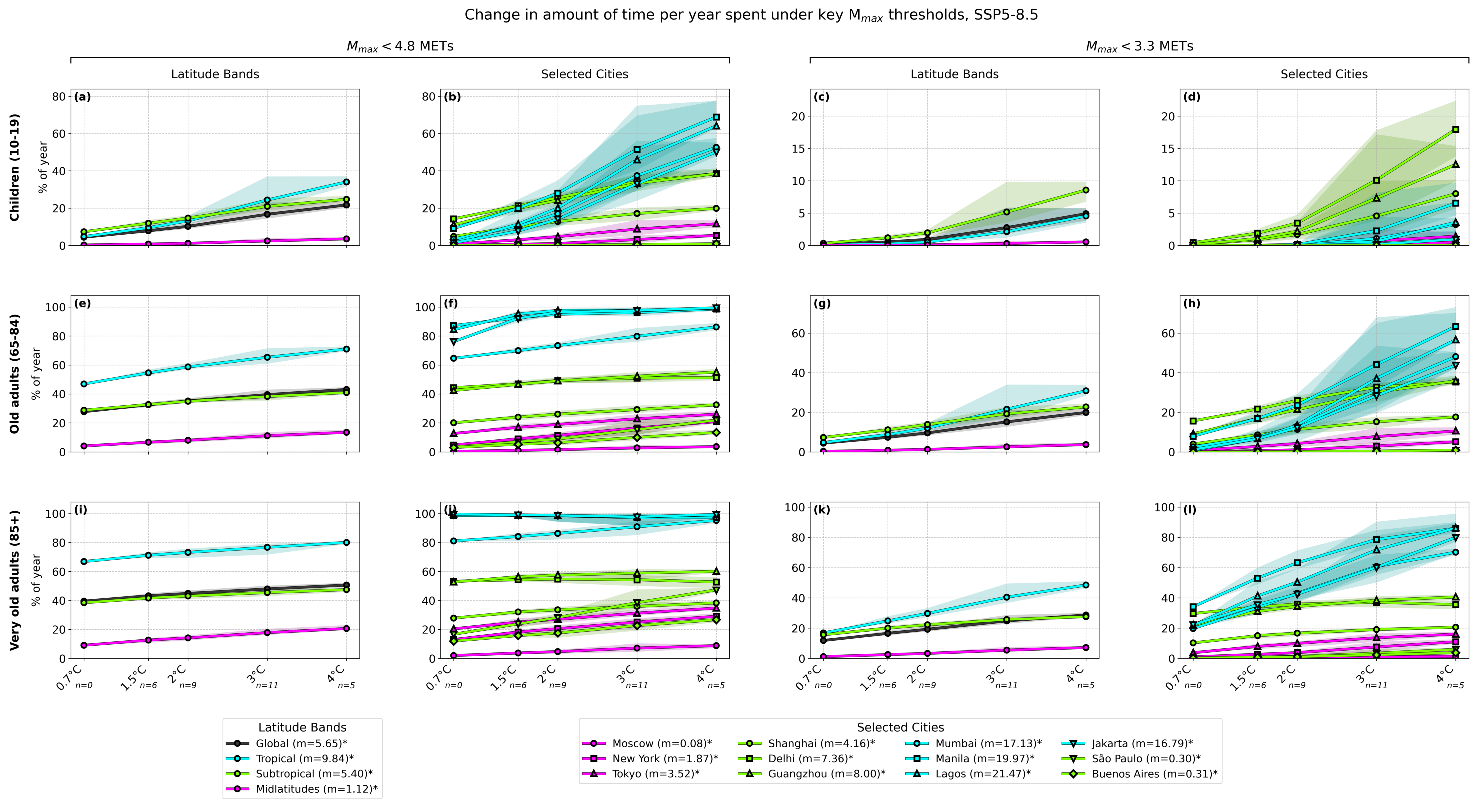

Fig. S3 As in Figure 2, but showing only the latitude-band and city line plots (without the accompanying maps) for three additional age-group profiles – children (10-19; a-d), old adults (65-84; e-h), and very old adults (85+; i-l) – under SSP5-8.5. Within each profile's row, panels are ordered bands then cities for the $M_{max} < 4.8$ METs threshold, followed by bands then cities for the $M_{max} < 3.3$ METs threshold. Adult (20-64) results are featured in Figure 2.

Within the tropics, the rate of increase in time spent under the $M_{max} < 4.8$ METs threshold per degree of GWL is smaller for old and very old adults than for adults (6.77%/°C and 3.64%/°C, respectively, versus 10.20%/°C for adults), despite elderly age groups still spending the largest overall share of the year under this threshold. This muted rate of increase likely reflects elderly individuals' reduced reliance on sweating for thermoregulation, which makes them comparatively less sensitive to the humidity increases accompanying tropical warming than younger adults and children. Elderly age groups also face substantial risk outside the tropics: in the subtropics, 34.96% and 43.08% of the year, on average, falls under the $M_{max} < 4.8$ METs threshold for old and very old adults, respectively, at a 2°C GWL.

Under the more moderate SSP2-4.5 scenario (Figure S4), tropical-band values at 2°C GWL are close to their SSP5-8.5 counterparts at the same GWL, consistent with global warming level (rather than emissions pathway or calendar year) being the primary control on M_{max}: for $M_{max} < 4.8$ METs, 13.09% (children), 37.57% (adults), 58.39% (old adults), and 73.72% (very old adults); for $M_{max} < 3.3$ METs, 0.51%, 2.83%, 11.91%, and 29.80%, respectively. Figure S5 shows this same SSP2-4.5 comparison in Figure 3's multi-profile pixel-plot layout; because SSP2-4.5 does not reach a 4°C GWL within the models considered in this analysis (Table S2), Figure S5 spans only four GWLs (baseline through 3°C).

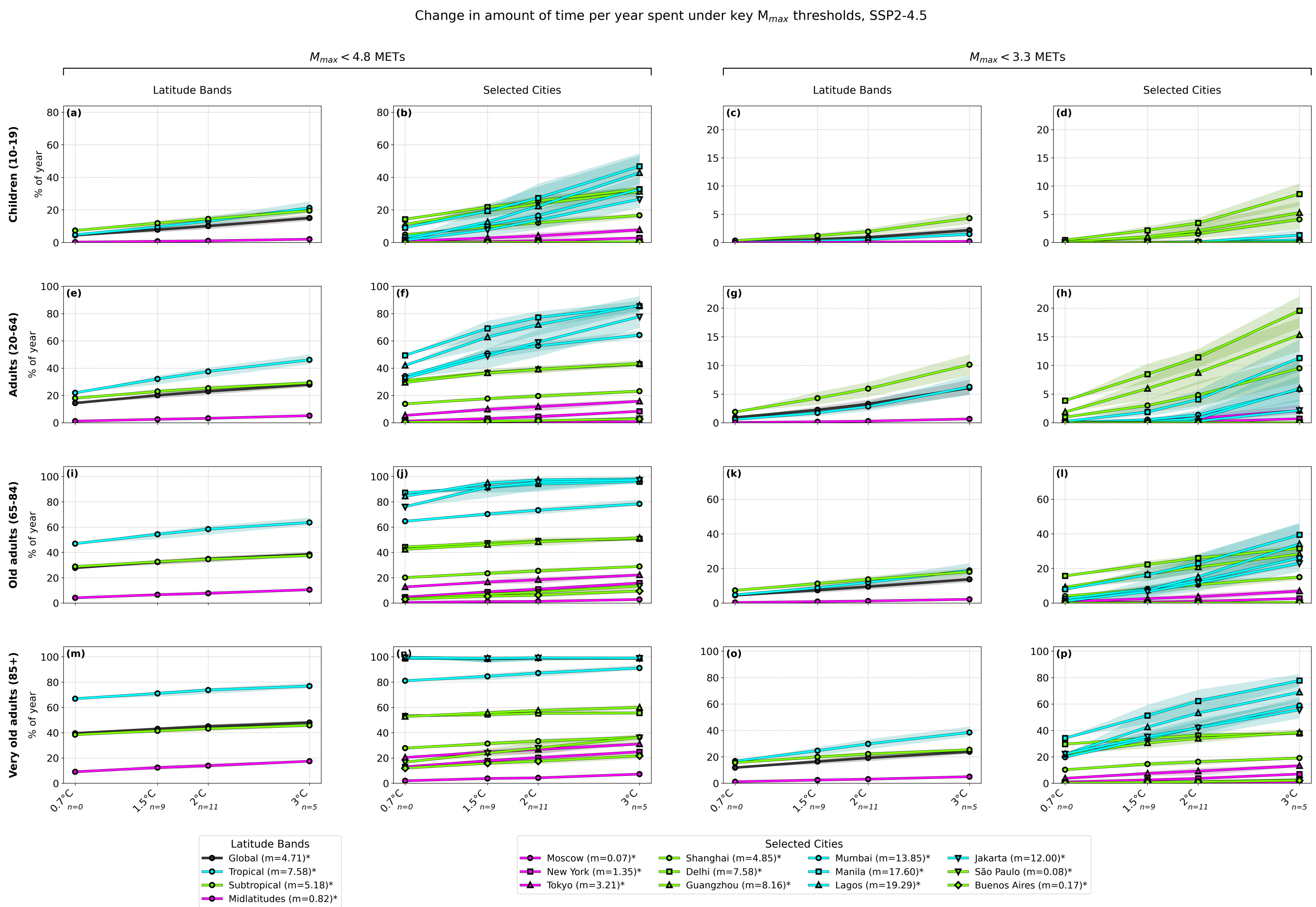

Fig. S4 As in Figure 2, but showing only the latitude-band and city line plots (without the accompanying maps) for all four age-group profiles – children (10-19; a-d), adults (20-64; e-h), old adults (65-84; i-l), and very old adults (85+; m-p) – under SSP2-4.5. Panel ordering within each row follows Figure S3.

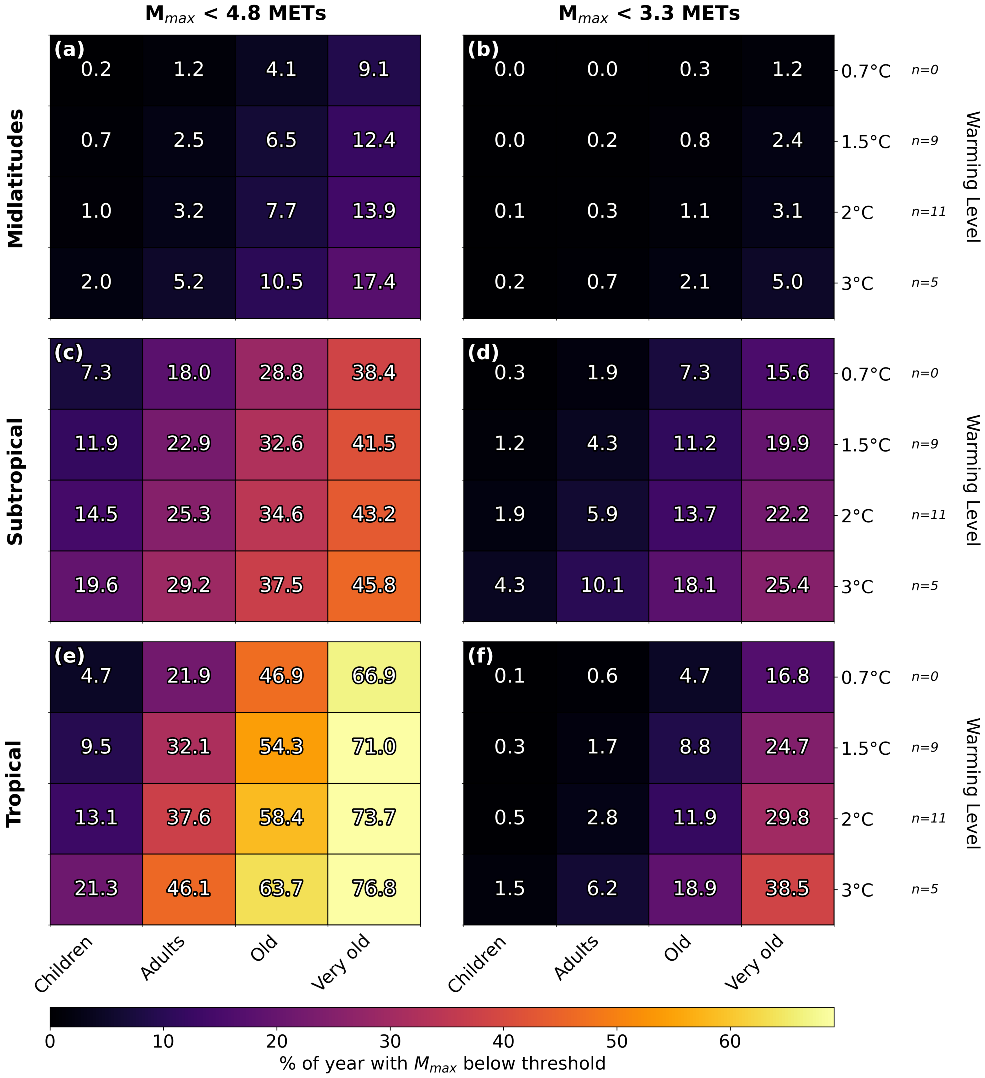

Fig. S5 As in Figure 3, but for SSP2-4.5.

1.3 Time of emergence of survivable-but-not-livable conditions (Figures S6–S7)

In addition to the 4.8 and 3.3 MET thresholds, we consider a very stringent threshold of $M_{max} < 1.5$ METs. Following Vanos et al, heat conditions at this level are considered survivable but "unlivable," with anything beyond minimal PA, such as doing light desk work, being uncompensable [2]. A grid cell is flagged as having reached this threshold at a given GWL once the multi-model-mean count of qualifying 3-hourly instants reaches at least one per year, averaged across that GWL's model ensemble. For children and adults, very few places on Earth experienced any < 1.5 METs conditions during the ERA5 climatology period with 0.7°C GWL (Figures S6a and S6b, yellow; 0% or 0.2% of all land grid cells, respectively). Children are able to accomplish at least 1.5 METs of compensable PA in most places of the world, even at a 4°C GWL (97.1% of land grid cells). However, at just 1.5°C GWL, adults will begin experiencing unlivable conditions in some tropical places (1.3% of all land grid cells). Large swaths of the tropics, the Americas, and Australia will see unlivable conditions for adults at 3°C or 4°C GWL (7.0% and 12.0% of all land grid cells, respectively).

For old and very old adults, large regions of the tropics and Australia already experience unlivable conditions during the historical baseline period (6.0% and 12.4% of land grid cells for old and very old adults, respectively). At 1.5°C GWL, unlivable conditions become common across low-elevation, lower-latitude regions for elderly age groups (13.8% and 23.6% of all land grid cells for old and very old adults, respectively). With 3°C or 4°C GWL, very old adults may see unlivable conditions even in high-latitude places within northern Canada and northern Russia. By 3°C or 4°C GWL, unlivable conditions will affect a substantial share of all land grid cells at some point in the year for very old adults (40.5% and 46.7% of land grid cells, respectively). The same emergence pattern holds under the more moderate SSP2-4.5 scenario (Figure S7, below).

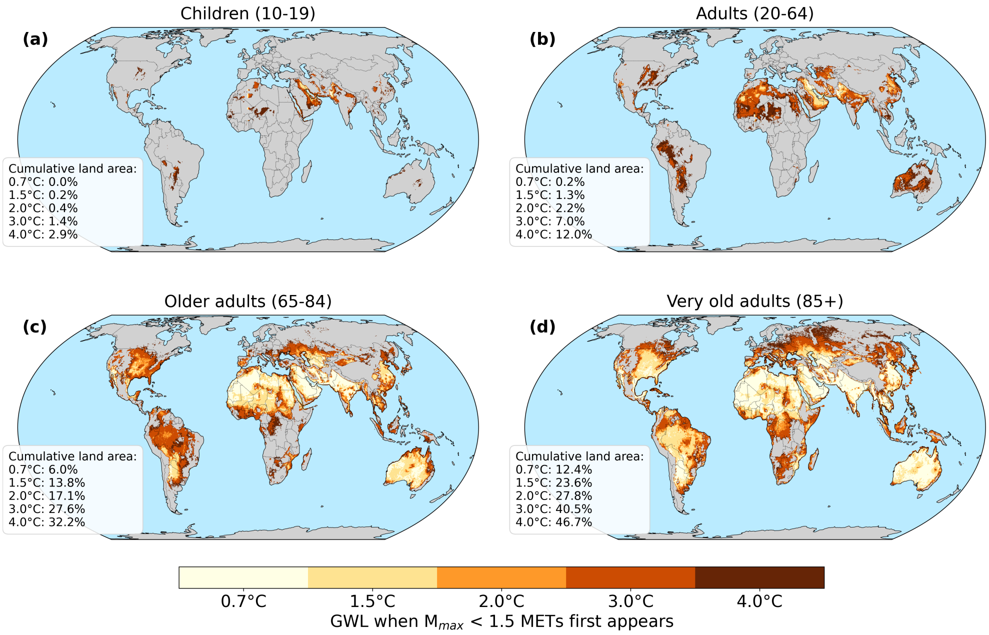

Fig. S6 Emergence of unlivable (M_{max} < 1.5 METs) conditions with climate change, SSP5-8.5. Lowest GWL where any amount of time in a grid cell, quantified via 3-hourly intervals, is spent with M_{max} < 1.5 METs for **a)** children (10-19), **b)** adults (20-64), **c)** old adults (65-84), and **d)** very old adults (85+). The percentage of land pixels that experience any amount of time where M_{max} < 1.5 METs at each GWL of interest is shown in the lower left of each subplot. Gray areas never experience M_{max} < 1.5 METs under any of the analyzed GWLs in the multi-model mean.

As in Figure S6, Figure S7 shows the lowest GWL at which any amount of time in a grid cell is spent with $M_{max} < 1.5$ METs ("unlivable" conditions), for the four age groups under SSP2-4.5. Baseline and 1.5°C cumulative land-area percentages closely match their SSP5-8.5 counterparts (e.g., 6.0% and 12.4% of land grid cells at baseline for old and very old adults, respectively, identical to the SSP5-8.5 values reported above since the ERA5 baseline does not depend on emissions scenario). By 3°C GWL – the highest GWL reached by any model under SSP2-4.5 in this analysis – cumulative land-area percentages are 0.8% for children, 4.0% for adults, 21.9% for old adults, and 34.6% for very old adults. Adults' value at 3°C is notably lower than the 7.0% reported for SSP5-8.5 at the same GWL above, likely reflecting the smaller and different set of models that reach 3°C under SSP2-4.5 (5 models) compared to SSP5-8.5 (11 models; Table S2).

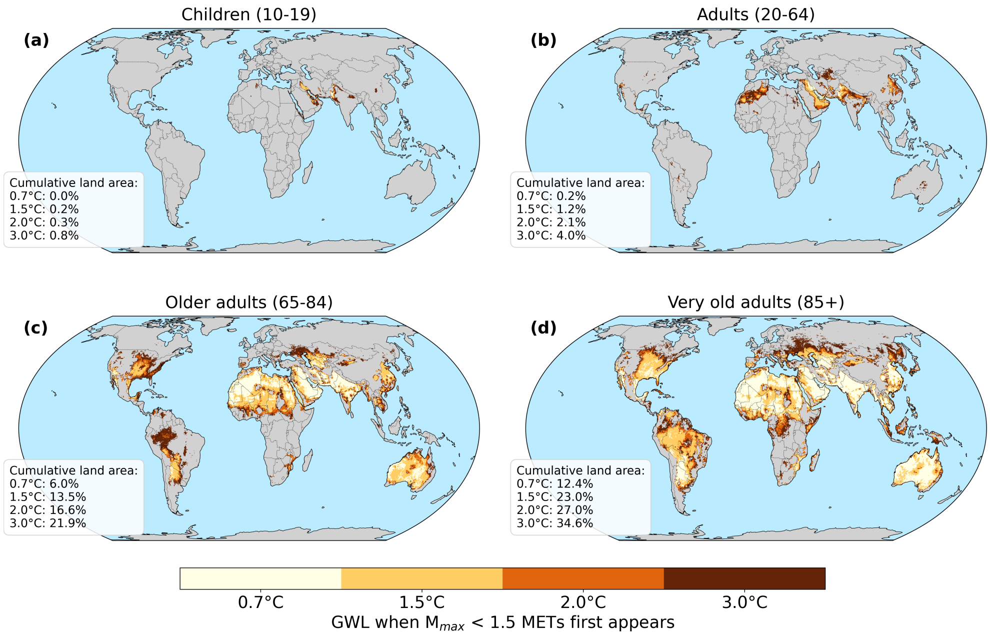

Fig. S7 As in Figure S6, but for SSP2-4.5.

1.4 Drivers of future person-hours risk under SSP2-4.5 (Figure S8)

As discussed in the main text (Results 2.3), Figure S8 presents the same person-hours (PH/yr) driver decomposition shown in Figure 4, but for the more moderate SSP2-4.5 scenario. Because SSP2-4.5 reaches each GWL later in calendar time than SSP5-8.5, and population and age-structure projections are matched to each model's own GWL-crossing year (Online Methods 4.5.2), the climate-change driver is nearly unchanged between scenarios at the same GWL (e.g., at 2°C GWL for the $M_{max} < 4.8$ METs threshold, ∼99.4 billion PH/yr (∼12.4 billion workdays/year) under SSP2-4.5 versus ∼102 billion PH/yr (∼12.7 billion workdays/year) under SSP5-8.5), while both demographic drivers are consistently larger under SSP2-4.5, since the same warming level is reached later in time when the population is larger and older. Combined, aging and population density account for a larger share of the total demographic-plus-climate effect under SSP2-4.5 than under SSP5-8.5 at every GWL and threshold considered: for the $M_{max} < 3.3$ METs threshold, 48.0%/47.5%/34.2% (SSP2-4.5, at 1.5°C/2°C/3°C GWL, respectively) compared to 45.4%/40.0%/30.0% (SSP5-8.5, same GWLs); for the $M_{max} < 4.8$ METs threshold, 67.5%/65.3%/56.4% (SSP2-4.5) compared to 64.3%/59.8%/50.6% (SSP5-8.5). SSP2-4.5 does not reach a 4°C GWL within the models considered in this analysis (Table S2), so no SSP2-4.5 value is available at that GWL.

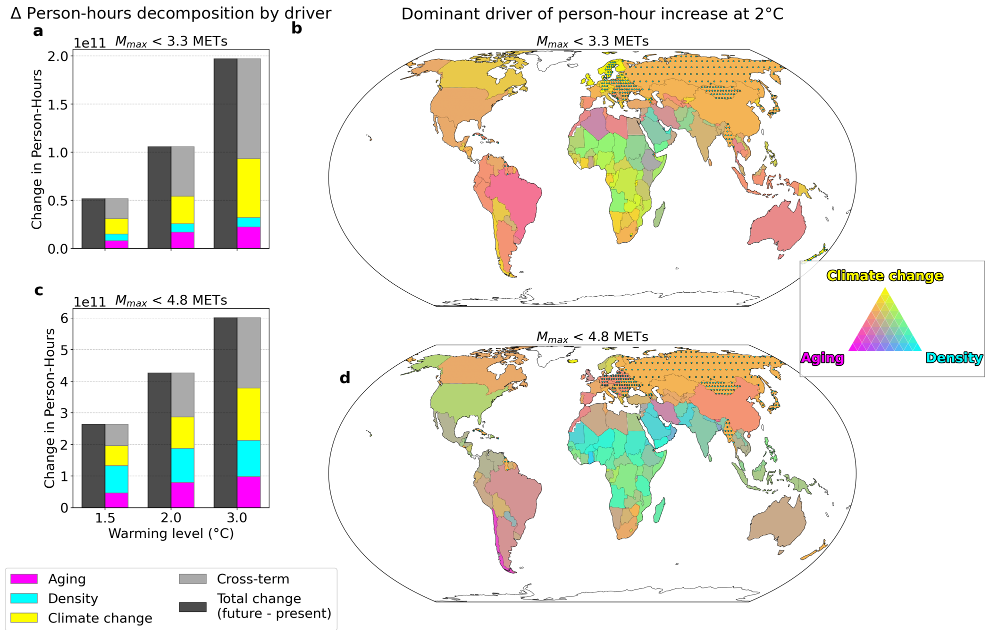

Fig. S8 As in Figure 4, but for SSP2-4.5.

This same later-crossing-year mechanism is visible in the total PH/yr figures for the $M_{max} < 3.3$ METs threshold: by its later 2°C-crossing year (on average, 2055, versus SSP5-8.5's 2042), global population under SSP2-4.5 is 10.9% higher than SSP5-8.5's population at its own, earlier 2°C-crossing year, so that total PH/yr under SSP2-4.5 modestly exceeds SSP5-8.5's ∼102 billion (629% increase) at the same nominal GWL. Table S1 reports the full set of total PH/yr and workday-equivalent values for both M_{max} thresholds under SSP2-4.5, as the SSP2-4.5 counterpart to Table 1 in the main text.

Table S1 Total person-hours per year (PH/yr) and workday-equivalents (workdays/yr), both in billions, under key M_{max} thresholds and global warming levels (GWL), for SSP2-4.5. Percent change is relative to the 1980-2010 ERA5 historical baseline (0.7°C GWL); baseline values are identical to Table 1 since the ERA5 baseline does not depend on emissions scenario. No SSP2-4.5 models reach a 4°C GWL within the model output available for this analysis (Table S2), so that GWL is omitted here.

	$M_{max} < 3.3$ METs			$M_{max} < 4.8$ METs		
GWL	PH/yr	Workdays/yr	% chg	PH/yr	Workdays/yr	% chg
Baseline (0.7°C)	13.9	1.74	–	195	24.4	–
1.5°C (avg. 2034)	65.8	8.22	+371%	459	57.4	+135%
2°C (avg. 2055)	120	15.0	+759%	621	77.7	+218%
3°C (avg. 2067)	211	26.4	+1413%	796	99.5	+307%

2 Supplementary Methods

2.1 Climate models

We use huss, ps, and tas from all models listed in Table S2. A model is included in this analysis for a given scenario only if it was availabe on the ESGF archive under that scenario at all; a model that is available under a scenario is further included at a given GWL only if it has a full climatology window centered on that GWL's crossing year (see Online Methods 4.3). Because models differ in how many years of output they provide and in when (or whether) they cross each GWL, the set of models actually contributing to the multi-model mean varies by GWL within a scenario, not just between scenarios – this is also why the number of models bracketed underneath the x-axis of Figures 1-3 changes across GWLs. Table S2 reports, for every model considered, which of the seven scenario/GWL combinations in this analysis it is included in.

Table S2 CMIP6 models included at each global warming level (GWL) and scenario combination. A checkmark (✓) indicates the model has a full climatology window centered on that GWL's crossing year and is included in the multi-model mean; a blank cell indicates the model is available under that scenario but lacks a full window at that GWL and is dropped (see Online Methods 4.3); an em dash (—) indicates the model is not run under that scenario at all. No SSP2-4.5 models reach a 4°C GWL within the model output available for this analysis, consistent with SSP2-4.5's lower-emissions trajectory, so that scenario/GWL combination is omitted here and not reported elsewhere in this work. All models use r1i1f1p1 output, except for FGOALS-g3 (marked †), which uses r3i1f1p1 output – this refers only to a different ensemble member, as r1 wasn't available. All model output is used at a frequency of 3hrPt (instantaneous sampling), except for GFDL-ESM4 (marked *), which instead provides huss, ps, and tas at a frequency of 3hr (three-hour averages).

	SSP5-8.5				SSP2-4.5		
Model	1.5°C	2°C	3°C	4°C	1.5°C	2°C	3°C
ACCESS-CM2	✓		✓	✓	✓	✓	✓
BCC-CSM2-MR	✓	✓	✓		✓	✓	
CanESM5-1			✓	✓	—	—	—
CMCC-CM2-SR5		✓	✓		✓	✓	✓
CMCC-ESM2	✓	✓	✓	✓	✓	✓	✓
EC-Earth3		✓	✓	✓		✓	✓
FGOALS-g3†	—	—	—	—	✓	✓	
GFDL-ESM4*	—	—	—	—	✓	✓	
KACE-1-0-G			✓	✓			✓
KIOST-ESM		✓	✓			✓	
MIROC6	✓	✓	✓		✓	✓	
MPI-ESM1-2-HR	✓	✓	✓		✓	✓	
MRI-ESM2-0	✓	✓	✓	✓	✓	✓	
Models included (n)	6	9	11	5	9	11	5

2.2 HEAT-Lim configuration

Table S3 HEAT-Lim configuration for different age groups.

	Children (10-19)	Young adults (20-64)	Old adults (65-84)	Very old adults (85+)
Mass (kg)	56.2	78	73.9	73.9
Body surface area (m2)	1.6	1.83	1.78	1.78
Sweat rate (L/hr)	0.75	0.75	0.51	0.51
Maximum skin wettedness (unitless)	0.85	0.85	0.65	0.49

HEAT-Lim can be configured for many different physiologies, corresponding to a diversity of humans. In this analysis, we modulate height, mass, body surface area, sweat rate, and maximum skin wettedness as proxies for four different age groups: children (10-19), young adults (20-64), old adults (65-84), and very old adults (85+) (Table S3). Note that these age groups are only general guidelines. In reality, height, mass, body surface area, and sweating ability do not have discontinuous changes at specific ages. As noted in the Online Methods, simplifying the entire world population to four subgroups requires making some coarse assumptions. However, we again note that this is still a substantive step beyond existing heat-impact projections.

A number of different sources were evaluated to determine appropriate values for each variable for each age group. We support the choices made in Vanos et al. 2023 and wished to reuse these profiles to maintain consistency within the literature. We concluded that the values of the "young woman" profile from Vanos et al. 2023 were close enough to be representative of children of both sexes aged 10-19; thus, our "children" profile is the exact same profile as the "female young adult" profile used elsewhere in the literature. Similarly, our "old adults" profile (ages 65-84) is the same as the female old adult profile used in Vanos et al. 2023. However, in choosing a body morphology for our "young adults" group, we recognized that using data based solely on female bodies would not be representative of the majority of the world population. Thus, we reevaluated the available data with both sexes in mind. Vanos et al. 2023 [1] consulted ExposFacts and the EPA Exposure Handbook (using NHANES data) to select mass and body surface area values for their representative "young" and "old" female adults [3, 4]. For this analysis, we additionally consulted a new CDC dataset [5]. We therefore increased the height and mass from the children/Vanos et al. 2023 values for our new "young adult" group to be representative of an average across both sexes and all datasets. Body surface area for this group was calculated using the Dubois-Dubois body surface area equation [6], using a height of 1.624 m alongside the mass reported in Table S3. Height is therefore not reported in Table S3 for the children, old adult, and very old adult profiles: their body surface area values are instead taken directly from the literature, so no corresponding height value was used for those groups. Maximum skin wettedness and sweat rate remain the same between "children" and "young adults," a decision based on recent analysis of children's sweating abilities [7–9].

We chose to maintain the body morphology from the "old adults" group for the "very old adults" group so that differences between the two groups could be attributed solely to differences in sweating constants. We additionally chose to maintain the sweat rate values across old adults, given that most heat chamber experiments in that age group are not set up to properly estimate maximum whole body sweat rate, as required in very hot, dry, and windy conditions to elicit the highest required heat loss via evaporation. The required heat loss via evaporation has been observed as the driver of sweating in this kind of experiment; as in Vanos et al. 2023, both the 0.75 and 0.51 values are based on results from Morris et al. 2019 [10]. More work has been done to estimate maximum skin wettedness across a variety of temperature-humidity conditions. We consulted studies from the PSU HEAT Project to estimate maximum skin wettedness for "very old adults" [11, 12]. Values from these studies for those aged 85+ were variable, with some individual data points showing maximum skin wettedness approaching zero. We chose a maximum skin wettedness of 0.49 for "very old adults" to represent a conservative estimate of decline in sweating ability in very old adults.

2.3 Driver decomposition of person-hours risk

This section expands on the person-hours (PH) driver-decomposition math introduced in Online Methods section 4.6, spelling out the isolated formula for each of the three drivers (climate change, population density, aging) underlying Figure 4.

As in Online Methods 4.6, PH risk in a grid cell for age group a at a given GWL is

$$P_a = H_a \times D \times R_a, \tag{1}$$

where H_a is the number of hours per year that M_{max} falls below the threshold of interest for age group a ("hot-hours"), D is population density (not age-specific), and R_a is the proportion of the grid-cell population in age group a. Total PH in a grid cell sums over the four age groups $a \in \{\text{children, adult, old, very old}\}$:

$$P_{total} = \sum_a P_a = \sum_a H_a \times D \times R_a. \tag{2}$$

To isolate the contribution of a single driver, P_{total} is recomputed allowing only that driver's variable (H_a, D, or R_a) to take its value at the future GWL of interest (2°C throughout Figure 4), while the other two variables are held at their ERA5 baseline (0.7°C) values; the baseline PH total is then subtracted to leave only that driver's effect. Online Methods 4.6 gives the climate-change-only term as a worked example. The density-only and aging-only terms are constructed the same way, varying D or R_a in place of H_a:

$$\begin{aligned} P_{total,\ climate\ change\ only} &= \sum_a H_{a,\ 2^\circ\mathrm{C}} \times D_{0.7^\circ\mathrm{C}} \times R_{a,\ 0.7^\circ\mathrm{C}} \\ &\quad - \sum_a H_{a,\ 0.7^\circ\mathrm{C}} \times D_{0.7^\circ\mathrm{C}} \times R_{a,\ 0.7^\circ\mathrm{C}} \end{aligned} \tag{3}$$

$$P_{total,\ density\ only} = \sum_a H_{a,\ 0.7^\circ\mathrm{C}} \times D_{2^\circ\mathrm{C}} \times R_{a,\ 0.7^\circ\mathrm{C}}$$

$$- \sum_a H_{a,\ 0.7^\circ\mathrm{C}} \times D_{0.7^\circ\mathrm{C}} \times R_{a,\ 0.7^\circ\mathrm{C}} \qquad (4)$$

$$P_{total,\ aging\ only} = \sum_a H_{a,\ 0.7^\circ\mathrm{C}} \times D_{0.7^\circ\mathrm{C}} \times R_{a,\ 2^\circ\mathrm{C}} - \sum_a H_{a,\ 0.7^\circ\mathrm{C}} \times D_{0.7^\circ\mathrm{C}} \times R_{a,\ 0.7^\circ\mathrm{C}} \qquad (5)$$

Because D is not age-specific, it takes the same value across all four age groups in every term; only H_a and R_a vary by age group. Each term is calculated per grid cell and then aggregated by country, restricted to grid cells with valid data in all three of the underlying demographic datasets (WorldPop for the baseline period; W22 and WIC for the future period; Online Methods 4.5.2). A country is excluded from this decomposition – and left unshaded in Figure 4b/d – if this shared valid-data domain covers less than 50% of the country's population (Section 2.4, Table S4).

The cross-term C (Figure 4a/c, light gray bars), representing nonlinear interactions among the three drivers, is the residual once the three individual driver terms (Eqs. 3–5) are subtracted from the full change in PH risk with all three drivers evolving together:

$$C = (P_{total,\ 2^\circ\mathrm{C}} - P_{total,\ 0.7^\circ\mathrm{C}}) - (P_{total,\ climate\ change\ only} + P_{total,\ density\ only} + P_{total,\ aging\ only}). \qquad (6)$$

Sign convention and country classification. For a given country, scenario, and M_{max} threshold, an individual driver term (Eqs. 3–5) can be negative – for example, $P_{total,\ density\ only}$ is negative for a country whose population is projected to decline. Figure 4b/d's ternary country maps encode only positive contributions to future risk, so before classifying a country, each term is floored at zero:

$$\tilde{P}_{total,\ i} = \max(P_{total,\ i},\ 0), \qquad i \in \{\text{climate change, density, aging}\}. \qquad (7)$$

A country's shading in Figure 4b/d is then set by the relative proportions of the three floored terms,

$$p_i = \frac{\tilde{P}_{total,\ i}}{\tilde{P}_{total,\ climate\ change} + \tilde{P}_{total,\ density} + \tilde{P}_{total,\ aging}}, \qquad \sum_i p_i = 1, \qquad (8)$$

used as ternary-color mixing weights (yellow for climate change, cyan for density, magenta for aging). Colored stippling over a country flags that the driver of the corresponding color had a negative raw contribution ($P_{total,\ i} < 0$) before flooring; because that driver's floored value is zero, it does not contribute to p_i or to the country's underlying shading.

2.4 Countries excluded from Figure 4 country-level driver maps

As described in Online Methods 4.6, the climate-change-only, density-only, and aging-only driver terms underlying Figure 4b/d are each built from demographic datasets (WorldPop, Wang et al. 2022, WIC) with different spatial coverage. Only grid cells with valid data in all three terms are used when computing each country's driver decomposition, and a country is left unshaded in Figure 4b/d if the resulting shared valid-data domain represents less than 50% of that country's population – otherwise, its driver classification would rest on an unrepresentative fraction of the population. Table S4 lists every country falling below this 50% threshold under at least one of the two emissions scenarios, along with its population-weighted coverage under each (bold indicates the scenario(s) in which the country is actually excluded). This affects Greenland, several small island nations, and a handful of other countries at 0.25° grid resolution where country boundaries leave little margin to begin with; none of these countries are discussed individually in the main text.

Coverage values differ between SSP5-8.5 and SSP2-4.5 but are identical between the two M_{max} thresholds for every country, because coverage depends only on where the underlying WorldPop/Wang et al. 2022/WIC population data are jointly valid, not on the M_{max} threshold applied there. It varies by scenario because each scenario's coverage is averaged over that scenario's own set of surviving models (Table S2) – a different set for SSP5-8.5 versus SSP2-4.5 – each matched to its own population-projection year at that model's individual GWL-crossing year (Online Methods 4.5.2); since SSP2-4.5 reaches 2°C later in calendar time than SSP5-8.5 on average, it draws on later population-projection snapshots overall, shifting the averaged coverage.

Table S4: Countries excluded from Figure 4b/d (left unshaded) because fewer than 50% of the country's population falls within the shared valid-data domain across the climate change, density, and aging driver terms (Online Methods 4.6). Population-weighted coverage is shown for each scenario; this coverage depends only on where the underlying population data are valid and does not vary between the two M_{max} thresholds (Section 2.4), so a single column suffices per scenario. A country is excluded from a given map only if its coverage falls below 50% for that scenario (all but Western Sahara are excluded under both).

Country	SSP5-8.5	SSP2-4.5
Antarctica	**0.0%**	**0.0%**
Bahamas	**9.9%**	**9.9%**
Brunei Darussalam	**27.4%**	**25.7%**
Cyprus	**8.3%**	**8.2%**
Falkland Islands / Malvinas	**0.0%**	**0.0%**
Fiji	**20.6%**	**19.9%**
French Southern and Antarctic Lands	**0.0%**	**0.0%**
Greenland	**4.2%**	**3.8%**
Haiti	**47.5%**	**47.4%**
Israel	**38.4%**	**39.3%**
Jamaica	**12.9%**	**12.8%**
Lebanon	**36.2%**	**36.9%**
Liberia	**46.5%**	**42.1%**
New Caledonia	**5.3%**	**5.0%**
Panama	**46.6%**	**47.0%**
Solomon Islands	**23.0%**	**23.2%**
Taiwan	**45.7%**	**44.5%**
Timor-Leste	**39.1%**	**35.5%**
Trinidad and Tobago	**17.8%**	**17.5%**

Table S4 – continued from previous page

Country	SSP5-8.5	SSP2-4.5
Vanuatu	**10.3%**	**9.3%**
Western Sahara	50.1%	**44.5%**

3 References

References

[1] Vanos, J. et al. A physiological approach for assessing human survivability and liveability to heat in a changing climate. *Nat. Commun.* **14**, 7653 (2023). https://www.nature.com/articles/s41467-023-43121-5

[2] Vanos, J. K., Baldwin, J. W., Jay, O. & Ebi, K. L. Simplicity lacks robustness when projecting heat-health outcomes in a changing climate. *Nat. Commun.* **11**, 6079 (2020). https://doi.org/10.1038/s41467-020-19994-1

[3] Zenie et al. 2026. https://data.jrc.ec.europa.eu/dataset/jrc-10114-10001

[4] US EPA. Exposure Factors Handbook, Chapter 8. https://www.epa.gov/system/files/documents/2025-01/efh-chapter08_508.pdf

[5] Fryer et al. 2025. *National Health Statistics Reports.* https://www.cdc.gov/nchs/data/series/sr_03/sr03-050.pdf

[6] Dubois, D. & Dubois, E. F. A formula to estimate the surface area if height and weight are known. *Arch. Intern. Med.* **17**, 863 (1916).

[7] Falk, B. & Dotan, R. Children's thermoregulation during exercise in the heat. *Appl. Physiol. Nutr. Metab.* (2008). https://cdnsciencepub.com/doi/10.1139/H07-185

[8] Tsuzuki, K. (2023). https://www.sciencedirect.com/science/article/pii/S0306456523000487

[9] Morris, N. B. et al. (2004). *Exp. Physiol.* https://physoc.onlinelibrary.wiley.com/doi/10.1113/expphysiol.2004.027979

[10] Morris, N. B., English, T., Hospers, L., Capon, A. & Jay, O. The Effects of Electric Fan Use Under Differing Resting Heat Index Conditions: A Clinical Trial. *Ann. Intern. Med.* **171**, 675–677 (2019). https://doi.org/10.7326/M19-0512

[11] Fisher, K. G., Vecellio, D. J., Cottle, R. M., Leach, O. K., Wolf, S. T. & Kenney, W. L. Lower maximal skin wettedness in both warm-humid and hot-dry environments with advanced age (PSU HEAT project). *J. Appl. Physiol.* **137**(6), 1549–1553 (2024). https://doi.org/10.1152/japplphysiol.00758.2024

[12] Fisher, K. G., Leach, O. K., Cottle, R. M. et al. Maximal skin wettedness as a function of environment and metabolic rate in unacclimated young and older adults (PSU HEAT Project). *Int. J. Biometeorol.* (2025). https://doi.org/10.1007/s00484-025-02986-5